

Magnetoresistance and Hall effect in epitaxial Co-Au superlattices

W. Vavra, C. H. Lee,* F. J. Lamelas, Hui He, Roy Clarke, and C. Uher
Department of Physics, The University of Michigan, Ann Arbor, Michigan 48109

(Received 15 February 1990; revised manuscript received 1 June 1990)

Resistivity, magnetoresistance, and the Hall effect have been measured in two epitaxially ordered Co-Au superlattices at temperatures between 2 and 295 K. One sample is composed of 60 bilayers of Co(5 Å)/Au(16 Å) and has a magnetic easy axis perpendicular to the film plane, while the other contains 30 bilayers of Co(30 Å)/Au(16 Å) and has an easy axis parallel to the film plane. The magnetoresistance effect of the first sample ($\sim 15\%$) is an order of magnitude larger than in the second sample. In addition, the Co(5 Å)/Au(16 Å) sample exhibits a large Hall voltage in zero applied magnetic field.

Ferromagnetic films based on ultrathin layers of $3d$ transition metals have recently aroused a great deal of attention due to their novel properties. Among these are the existence of large perpendicular anisotropies,¹ "giant" magnetoresistance effects,² and previously unobserved oscillations in the coupling of adjacent ferromagnetic layers.³ It has become evident that magnetotransport properties are quite sensitive to changes in the magnetic state and are a valuable tool for studying these systems. To date, however, there has been no direct comparison of transport properties between superlattice structures of similar composition but with out-of-plane versus in-plane magnetic easy axes. In this paper we show that the magnetoresistance and Hall effect are dramatically different for the two magnetic configurations.

Two samples were grown by molecular-beam epitaxy on (110)GaAs with a 500-Å epitaxial buffer layer of (110)Ge. The first sample consists of 60 bilayers of Co(5 Å)/Au(16 Å), and the second contains 30 bilayers of Co(30 Å)/Au(16 Å). Superconducting quantum interference device (SQUID) magnetometer measurements⁴ show that the first sample has an easy axis perpendicular to the film plane, whereas the film plane is an easy plane in the second sample. Measurements performed on a series of Co-Au samples⁴ show that a perpendicular easy axis occurs for Co layer thicknesses of less than 19 Å. Growth conditions and structural characterization (reflection high-energy electron diffraction, x-ray scattering, high-resolution transmission electron microscopy, and selected area diffraction) of the samples have been described elsewhere.¹

For the transport measurements discussed here, uniform current channels were obtained by photolithographically etching the superlattice films into a standard bridge pattern suitable for four-probe resistivity and Hall-effect measurements. This etch process reproduces sample dimensions to within 1 μm . The current channel on the film plane is 1 mm wide and parallel to the Au[2 $\bar{2}$ 0] and Co[11 $\bar{2}$ 0] axes. Wires were attached with indium and all measurements were performed with a dc technique using Keithley Model 181 nanovoltmeters.

The resistivity parallel to the plane of the Co(5 Å)/Au(16 Å) sample is 26.7 $\mu\Omega\text{cm}$ at 272 K, and 17.4

$\mu\Omega\text{cm}$ at 1.7 K. The corresponding values for the Co(30 Å)/Au(16 Å) structure are 17.9 and 11.7 $\mu\Omega\text{cm}$. The data refer to the as-grown multilayers that have not been exposed to a magnetic field. The absence of any nonmetallic behavior in the (low) temperature dependence of the resistivity is consistent with high quality interfaces in the structures. Nevertheless, the role the interfaces play in limiting the mean free path is evident from the 50% higher resistivity in the Co(5 Å)/Au(16 Å) structure relative to the Co(30 Å)/Au(16 Å) sample. For reference, the bulk resistivity at room temperature of single-crystal Au is 2.03 $\mu\Omega\text{cm}$ and it is 5.0 $\mu\Omega\text{cm}$ for single-crystal hcp Co measured perpendicular to the c axis.⁵

Magnetoresistance (MR) was measured in three different magnetic-field configurations: perpendicular MR where \mathbf{H} is applied normal to the film plane, longitudinal MR where \mathbf{H} is parallel to both the sample plane and the current \mathbf{J} , and transverse MR where \mathbf{H} is parallel to the sample plane but perpendicular to \mathbf{J} . Prior to data collection the samples were subjected to a saturating field.

A typical perpendicular MR plot is shown in Fig. 1. The effect of the anisotropy is seen in the large MR and hysteresis of the Co(5 Å)/Au(16 Å) superlattice. There are two interesting features in the MR of this sample. The first is that as the applied field is decreased from 35 kOe the resistance curves diverge at about 20 kOe. This is unexpected since magnetometer and Hall-effect measurements show that the saturation field is ~ 5.4 kOe. The second feature is the maximum in the MR which occurs at $H=3.6$ kOe at 4.2 K. This does not coincide with the value of the coercivity field $H_c=1.7$ kOe obtained from SQUID magnetometer data. In contrast, previous measurements^{6,7} of perpendicular MR in Au/Co/Au sandwiches have revealed a MR peak which lies within $\sim 15\%$ of H_c [H_c is defined as $H(M=0)$ where M is the magnetization]. We conclude that the MR peak does not necessarily coincide with $M=0$ in *multilayer* structures. This can be understood in terms of the different resistivities for the two electron spin states. With respect to the direction of \mathbf{M} , the scattering rates for spin-up and spin-down electrons are considerably different,⁸ and there is now strong experimental^{2,9} and theoretical¹⁰ evidence that this difference is an important mechanism for the electron

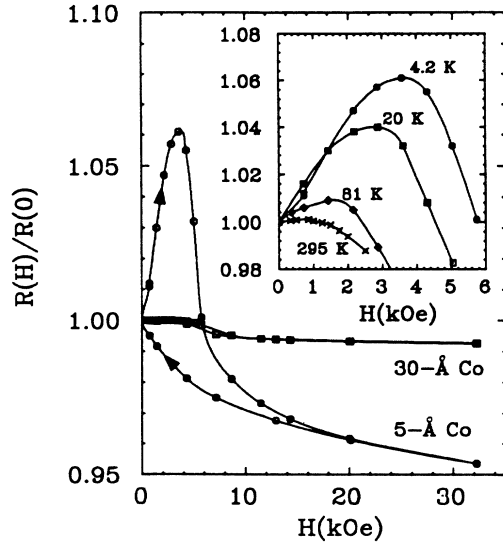


FIG. 1. Perpendicular magnetoresistance at 4.2 K. Inset shows temperature dependence of the resistance peak for the Co(5 Å)/Au(16 Å) sample.

transport in layered magnetic structures. The essential conclusion from Refs. 2, 9, and 10 is that the resistance is maximum when the number of boundaries between neighboring magnetic layers with antiparallel moments is maximum. To illustrate how this pertains to our data, several schematic cross sections are shown in Fig. 2. Figures 2(a) and 2(b) both correspond to $M=0$, but 2(a) contains one boundary between regions of opposite \mathbf{M} and therefore has a lower resistance than 2(b) which has three boundaries. Figure 2(c) shows an unequal number of up and down layers ($M \neq 0$), but it has a higher resistance than 2(a) since it contains two boundaries. Thus, the MR peak will not necessarily coincide with H_c .

The longitudinal and transverse MR (Fig. 3) are also markedly different in the two samples. The Co(30 Å)/Au(16 Å) superlattice displays behavior typical of a ferromagnet where a spin-orbit interaction¹¹ results in different resistivities for \mathbf{M} parallel or perpendicular to the current \mathbf{J} . The resistivities for these two cases are denoted by ρ_{\parallel} and ρ_{\perp} , respectively. In general, ρ_{\parallel} is greater than ρ_{\perp} , as is the case in the sample with Co(30 Å) layers. We note also that the longitudinal and transverse MR of this sample becomes nearly constant at the saturation field H_s . In contrast, the MR of the Co(5 Å)/Au(16 Å) sample is entirely different. The change in resistance with increasing field is an order of magnitude larger than in the Co(30 Å)/Au(16 Å) sample. Moreover, the resistivity decreases regardless of whether \mathbf{M} is perpendicular or parallel to \mathbf{J} which indicates a dominant mechanism other than the spin-orbit interaction of Ref. 11.

We now turn our attention to the Hall-effect data. The Hall resistivity of a magnetic material is given by¹²

$$\rho_H \equiv \frac{tV_H}{I} = R_o[H + 4\pi M_{\perp}(1 - N_{\perp})] + R_s 4\pi M_{\perp}, \quad (1)$$

where R_o and R_s are the ordinary and spontaneous Hall coefficients, V_H is the Hall voltage, I is the sample

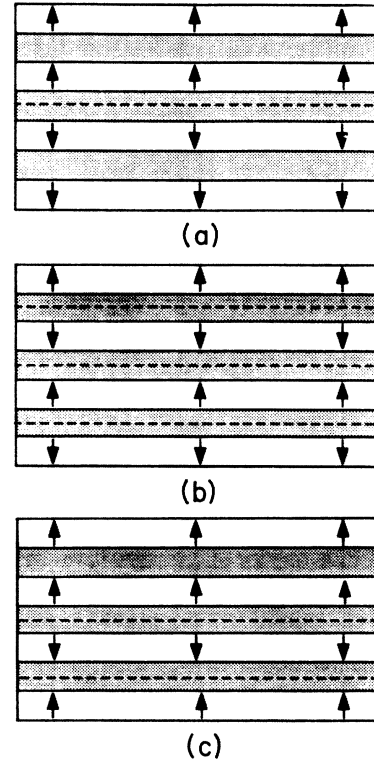


FIG. 2. Schematic cross section showing several possible magnetic ordering configurations. All shaded areas represent nonmagnetic spacer layers. The shaded areas with dashed lines denote spacer layers between antiparallel magnetic layers. (a) and (b) both have $M=0$ but (b) has more boundaries between antiparallel layers and therefore has higher resistance. (c) has $M \neq 0$ but has two antiparallel boundaries and a higher resistance than (a).

current, H is the magnetic field applied perpendicular to the film plane, M_{\perp} is the component of magnetization perpendicular to the film plane, N_{\perp} is the demagnetization factor perpendicular to the film, and t is the thickness of the structure. In contrast to cubic metals, the demagnetization factors for few-monolayer hexagonal structures

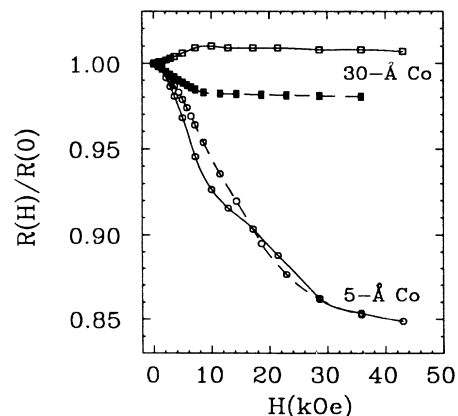


FIG. 3. Longitudinal and transverse (dashed line) magnetoresistance of Co(5 Å)/Au(16 Å) and Co(30 Å)/Au(16 Å) samples at 4.2 K.

differ very little from their continuum values,¹³ therefore we take $N_{\perp} = 1$ and

$$\rho_H = R_o H + R_s 4\pi M_{\perp}. \quad (2)$$

This means there will be a change in slope when M_{\perp} reaches saturation, and that a component of the magnetization perpendicular to the film will produce a Hall voltage even when $H = 0$.

The Hall resistivity versus applied field for three temperatures is shown in Fig. 4. The large Hall voltage at $H = 0$ provides an immediate confirmation of the perpendicular magnetization of the Co(5 Å)/Au(16 Å) sample. The sharpness of the transitions when M_{\perp} saturates and the linearity of the data above saturation indicate the samples are firmly magnetized along the c axis and high-field susceptibility corrections to Eq. (2) are not needed. The saturation field H_s , as determined by the intersection of the two linear parts of each plot, is strongly temperature dependent in the Co(5 Å)/Au(16 Å) sample and nearly temperature independent for the other sample. The values of H_s from Hall-effect measurements are listed in Table I and are in very good agreement with SQUID magnetometer measurements.

The two known mechanisms responsible for the spontaneous Hall effect in magnetic materials are *skew scattering* which is generally dominant below 100 K and *side jump* above 100 K.^{8,14,15} The contribution from each

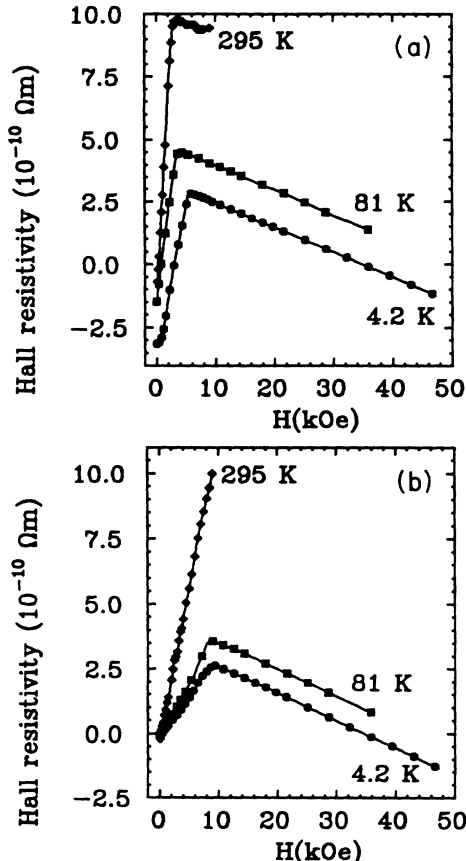


FIG. 4. Hall resistivity for samples of (a) Co(5 Å)/Au(16 Å) and (b) Co(30 Å)/Au(16 Å).

TABLE I. Temperature dependence of saturation field from Hall-effect measurements.

Temperature	H_s from Hall effect	
	5-Å Co	30-Å Co
4.2 K	5370 (Oe)	9050
81	3430	9000
295	2660	~9000

mechanism can be determined by comparing R_s with the sample resistivity. The skew-scattering theory predicts $R_s \propto \rho$, while for the side jump mechanism $R_s \propto \rho^2$. For our two samples this is equivalent to determining

$$n = \frac{\ln(R_{s1}/R_{s2})}{\ln(\rho_1/\rho_2)}, \quad (3)$$

where n is the exponent of ρ and we use the value of ρ after the samples have been magnetized perpendicular to the film plane. To extract R_s from the data of Fig. 4 we need M_{\perp} as a function of H . The magnetometer hysteresis loops show that M_{\perp} increases linearly from $H = 0$ to near saturation, therefore, we take $M_{\perp} = \chi H + c$, where χ is read from the hysteresis loop and c is a constant. The slope of the Hall resistivity below saturation is now given by $R_o + R_s 4\pi \chi$ which can be solved for R_s and then inserted into Eq. (2). Using the total superlattice thickness¹⁶ for t in Eq. (1) yields $n = 0.83$ and 1.39 at 4.2 and 81 K, consistent with the predicted temperature dependence. The value of n at 295 K was not determined.

Recent progress in the growth of multilayer structures has reopened the issue of surface or interface contributions to magnetic anisotropy.⁴ It is not clear how the original ideas¹⁷ of surface anisotropy apply to these new materials. Therefore, it is of interest to estimate the surface anisotropy using the saturation field from Hall-effect measurements. The anisotropy energy density for a thin film with the hexagonal axis and the applied field perpendicular to the film plane can be written¹⁸

$$E = -M_{\perp} H + 2\pi M_{\perp}^2 + \left[K_{ME} - K_1 + \frac{2K_s}{t_{Co}} \right] \left(\frac{M_{\perp}}{M_s} \right)^2. \quad (4)$$

The first term is the interaction energy between the magnetization and the external field, the second term is the demagnetization energy, K_{ME} and K_1 are the magnetoelastic and magnetocrystalline¹⁹ anisotropy constants. The last term is the surface anisotropy with the form and sign convention of Néel.¹⁷ Minimization of the energy density ($\partial E / \partial M_{\perp} = 0$) at saturation gives

$$H_s = 4\pi M_s + \frac{2}{M_s} (K_{ME} - K_1) + \frac{4K_s}{M_s t_{Co}}. \quad (5)$$

The magnetoelastic energy density is

$$E_{ME} = - \left[c_{11} + c_{12} - 2 \frac{c_{13}^2}{c_{33}} \right] (\lambda_A + \lambda_B) \epsilon \sin^2 \theta \\ \equiv -K_{ME} \sin^2 \theta. \quad (6)$$

The c 's and λ 's are elastic²⁰ and magnetostriction²¹ constants, and ϵ is the epitaxial strain within the film plane. The Co strain in the Co(30 Å)/Au(16 Å) sample as measured by in-plane x-ray scattering was found to be $\epsilon = 0.0042$ at 295 K. [Due to limitations in x-ray intensity the strain in the Co(5 Å)/Au(16 Å) sample is not presented.] This yields $K_{ME} = -2.74 \times 10^6$ ergs/cm³, and from Ref. 20 the room-temperature value of K_1 is 4.12×10^6 ergs/cm³. SQUID magnetometer measurements indicate that M_s in the Co(30 Å)/Au(16 Å) sample is 1300 emu/cm³, i.e., 90% of the bulk Co value. The leading terms²² of K_1 , λ_A , and λ_B are proportional to M_s^2 , therefore, these parameters will be reduced to $0.9^2 = 81\%$ of their bulk values. Using the reduced parameters, Eq. (5) yields $K_s = 0.12$ ergs/cm². Given the uncertainties in the measurements of the terms in Eq. (5) this value is not significantly different from zero. This is consistent with the magnetometer measurements of Ref. 4, where we show that the magnetoelastic term, rather than a large surface anisotropy, is important in accounting for the strong perpendicular anisotropy in our epitaxial Co-Au superlattices.

In summary, we have shown that the magnetoresistance and Hall effect of epitaxial Co-Au superlattices vary

dramatically depending on the orientation of the magnetic easy axis. If the easy axis is perpendicular to the film plane the magnetoresistive anisotropy typical of a ferromagnet is not observed, and the perpendicular magnetoresistance is hysteretic. Moreover, the longitudinal, transverse, and perpendicular magnetoresistance effects are an order of magnitude larger when the easy axis is perpendicular to the film plane than when it lies in the plane. Hall-effect measurements allow accurate determination of the saturation fields for either orientation of the easy axis, and the presence of a perpendicular magnetization is readily confirmed by a nonzero Hall voltage in zero applied magnetic field.

We are particularly grateful for discussions with R. E. Camley and A. B. Kaiser, and acknowledge the assistance of R. Richardson and S. Elagöz. This research was supported in part by National Science Foundation Low Temperature Physics Grant No. DMR-8805156, and by National Science Foundation Materials Research Grant No. DMR-8905367. One of us (F.L.) was partially supported by the U.S. Army Research Office under Grant No. DAAL-03-86-G-0053.

*Present address: IBM Almaden Research Center, K32/803 San Jose, CA 95120.

¹C. H. Lee, Hui He, F. Lamelas, W. Vavra, C. Uher, and Roy Clarke, *Phys. Rev. Lett.* **62**, 653 (1989).

²M. N. Baibich, J. M. Broto, A. Fert, F. Nguyen Van Dau, F. Petroff, P. Etienne, G. Creuzet, A. Friederich, and J. Chazelas, *Phys. Rev. Lett.* **61**, 2472 (1988).

³S. S. P. Parkin, N. More, and K. P. Roche, *Phys. Rev. Lett.* **64**, 2304 (1990).

⁴C. H. Lee, Hui He, F. Lamelas, W. Vavra, C. Uher, and Roy Clarke, *Phys. Rev. B* **42**, 1066 (1990).

⁵J. Bass, in *Landolt-Bornstein Tables III*, edited by K.-H. Hellwege and J. L. Olsen (Springer-Verlag, Berlin, 1982), Vol. 15a.

⁶E. Vélú, C. Dupas, D. Renard, J. P. Renard, and J. Seiden, *Phys. Rev. B* **37**, 668 (1988). This reference does not contain magnetometer data.

⁷P. Beauvillain, P. Bruno, C. Chappert, C. Dupas, F. Trigui, E. Vélú, and D. Renard, *J. Phys. C* **8**, 1703 (1988).

⁸I. A. Campbell and A. Fert, in *Ferromagnetic Materials*, edited by E. P. Wohlfarth (North-Holland, Amsterdam, 1982), Vol. 3.

⁹G. Binasch, P. Grünberg, F. Saurenbach, and W. Zinn, *Phys. Rev. B* **39**, 4828 (1989).

¹⁰R. E. Camley and J. Barnaś, *Phys. Rev. Lett.* **63**, 664 (1989).

¹¹I. A. Campbell, A. Fert, and O. Jaoul, *J. Phys. C* **3**, Suppl. S95 (1970).

¹²S. M. Hurd, *The Hall Effect in Metals and Alloys* (Plenum, New York, 1972), p. 158.

¹³M. Farle, A. Berghaus, and K. Baberschke, *Phys. Rev. B* **39**, 4838 (1989).

¹⁴P. Nozières and C. Lewiner, *J. Phys.* **34**, 901 (1973).

¹⁵L. Berger, *Phys. Rev. B* **2**, 4559 (1970).

¹⁶A reasonable approach would be to take t as the total Co thickness and then subtract the Hall coefficient R_o of bulk Au from the resulting ρ_H . But, to be consistent, the resistivity of the Co layers alone should be used in the denominator of Eq. (3). M. Gurvitch [*Phys. Rev. B* **34**, 540 (1986)] has developed a technique to extract the resistivity of individual layers of a metallic multilayered structure, however, if the layers are too thin his equations do not have a solution and unfortunately this is the case for our samples. Consequently we use the total superlattice thickness.

¹⁷L. Néel, *J. Phys.* **4**, 225 (1954).

¹⁸R. M. Bozorth, *Ferromagnetism* (Van Nostrand, New York, 1951), Chap. 18. The higher-order magnetocrystalline terms $K_2 \sin^4 \theta$ and $K_3 \sin^6 \theta$ have been omitted in Eq. (4) since they do not contribute to Eq. (5).

¹⁹J. D. Sievert and V. V. Zehler, *Z. Angew. Phys.* **30**, 251 (1970).

²⁰H. J. McSkimin, *J. Appl. Phys.* **26**, 406 (1955).

²¹A. Hubert, W. Unger, and J. Kranz, *Z. Phys.* **224**, 148 (1969).

²²W. P. Mason, *Phys. Rev.* **96**, 302 (1954).

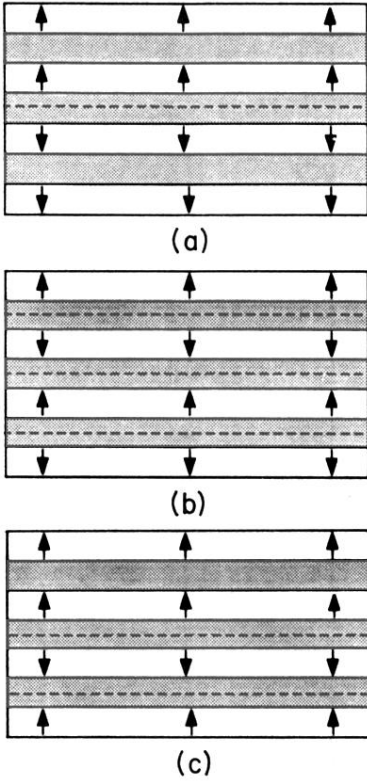


FIG. 2. Schematic cross section showing several possible magnetic ordering configurations. All shaded areas represent nonmagnetic spacer layers. The shaded areas with dashed lines denote spacer layers between antiparallel magnetic layers. (a) and (b) both have $M=0$ but (b) has more boundaries between antiparallel layers and therefore has higher resistance. (c) has $M \neq 0$ but has two antiparallel boundaries and a higher resistance than (a).